NASA CONTRACTOR REPORT

NASA CR-1254

EXPERIMENTAL INVESTIGATION OF ADVANCED CONCEPTS TO INCREASE TURBINE BLADE LOADING

III. Performance Evaluation of Tandem Rotor Blade

by H. G. Lueders

Prepared by
GENERAL MOTORS
Indianapolis, Ind.
for Lewis Research Center

NATIONAL AERONAUTICS AND SPACE ADMINISTRATION • WASHINGTON, D. C. • DECEMBER 1968

NASA CR-1254

EXPERIMENTAL INVESTIGATION OF ADVANCED CONCEPTS TO INCREASE TURBINE BLADE LOADING

III. Performance Evaluation of Tandem Rotor Blade

By H. G. Lueders

Prepared under Contract No. NAS 3-7902 by
ALLISON DIVISION, GENERAL MOTORS
Indianapolis, Ind.

for Lewis Research Center

NATIONAL AERONAUTICS AND SPACE ADMINISTRATION

For sale by the Clearinghouse for Federal Scientific and Technical Information
Springfield, Virginia 22151 – CFSTI price $3.00

FOREWORD

The research described herein, which was conducted by the Allison Division of General Motors, was performed under NASA Contract NAS3-7902. The work was done under the project management of Mr. Edward L. Warren, Airbreathing Engines Division, NASA-Lewis Research Center, with Mr. Richard L. Roelke, Fluid System Components Division, NASA-Lewis Research Center, as research consultant. The report was originally issued as Allison Division, General Motors EDR 4909, Volume III, July 1968.

ABSTRACT

The overall performance of a single-stage turbine designed with a tandem rotor blade and negative rotor hub reaction was investigated over a range of equivalent speeds and expansion ratios. Surveys of total pressure, flow angle, temperature, and hot-wire data were taken at the rotor trailing edge. The performance of the turbine is compared with the performance of a plain rotor blade turbine. Both turbines have the same design requirements and were tested with the same stator.

TABLE OF CONTENTS

EXPERIMENTAL INVESTIGATION OF ADVANCED CONCEPTS TO INCREASE TURBINE BLADE LOADING

III. PERFORMANCE EVALUATION OF TANDEM ROTOR BLADE

by H. G. Lueders

Allison Division, General Motors

SUMMARY

The overall performance of a single-stage turbine with a tandem rotor blade assembly was investigated over a range of equivalent speeds and expansion ratios. The tandem rotor blade was designed with negative rotor hub reaction. Rotor exit surveys were taken of total pressure, flow angle, temperature, and hot-wire data. The results of this investigation are compared with the performance of a plain rotor blade designed to the same aerodynamic requirements. Both rotors were tested using the same stator.

The total efficiency at design equivalent speed and pressure ratio was 87.6 percent compared to the plain blade performance of 88.4 percent. At corresponding expansion ratios, the tandem blade turbine had slightly higher efficiency at speeds greater than design and lower efficiency at reduced speeds. Static pressure measurements taken at the stator and rotor hub exits at design speed indicated negative reaction over the entire range of expansion ratio investigated. The plain blade hub reaction was only slightly higher, but still negative, than the tandem blade to an expansion ratio of 1.9; however, the reaction was positive at expansion ratios greater than 2.1. At this and greater expansion ratios, the plain blade was choked, while the tandem blade rotor did not choke over the range of expansion ratio investigated.

INTRODUCTION

The analysis and optimization of propulsion systems have always involved a balance or trade between (1) turbine efficiency and (2) turbine size and weight reduction. Generally, the reduction of turbine diameter, solidity, and/or stage reaction results in a smaller and/or lighter turbine but at some sacrifice in efficiency because of losses associated with increased blade loading. If the size and weight reduction can be accomplished without a loss in efficiency, considerable gains are available to the overall propulsion system.

NASA has initiated a program to investigate concepts to increase turbine blade loading without the associated losses currently encountered. The first

phase of the test program consisted of the testing of a plain rotor blade which had high suction surface diffusion. The performance of this blade, which forms the program base line, is presented in reference 1. For comparison, the following three different blading concepts are being evaluated:

- Vortex generators, often called boundary layer trip devices
- Tandem airfoil
- Jet flap

The analyses and design of these concepts are presented in reference 2. The tangential jet blade described in reference 2 is not scheduled for testing at this time because of vibrational problems. The tandem blade shown in Figure 1 is the subject of this report.

The tandem blade is composed of two airfoils which are designed to meet the same aerodynamic requirement as the conventional plain blade discussed in references 1 and 2. Highly loaded single-airfoil blades generate excessive boundary layer thickness in adverse pressure gradients which cause flow separation and high loss. The design philosophy of the tandem blade is to distribute the overall turning between two airfoils. This allows each airfoil to start its part of the turning process with a new thin boundary layer preventing boundary layer buildup and flow separation. The test results of a single-stage turbine with a tandem blade rotor installed are presented herein, including a comparison with the plain blade results of reference 1.

Performance data were taken from 70 to 110 percent of design equivalent speed in increments of 10 percent over a range of expansion ratios from 1.4 to a level near limiting loading. Limiting loading could not be achieved at the 100 and 110 percent equivalent speeds because of excessive blade vibratory stress at high expansion ratios.

Rotor exit surveys were conducted at the design equivalent speed and expansion ratio. Circumferential traverses with a combination total pressure, temperature, and yaw angle probe were made at constant radii to map the flow characteristics at the rotor trailing edge. A hot-wire anemometer survey was also made at the rotor trailing edge to provide additional insight to the rotor exit flow characteristics.

All testing was conducted while operating the test rig with inlet conditions of approximately 2.7 atmospheres absolute pressure and 650°R temperature.

SYMBOLS

E	specific work output, Btu/lb
$\dot{m}$	mass flow rate, lb/sec
N	rotational speed, rpm
P	pressure, psia
T	temperature, °R
ur	blade tangential velocity, ft/sec
V	absolute gas velocity, ft/sec
W	relative gas velocity, ft/sec
Γ	torque, ft-lb
δ_o	ratio of inlet air total pressure to standard sea level conditions
ϵ	function of γ defined as $\frac{\gamma^*}{\gamma} \frac{\left(\frac{\gamma+1}{2}\right)^{\gamma/(\gamma-1)}}{\left(\frac{\gamma^*+1}{2}\right)^{\gamma^*/(\gamma^*-1)}}$
η_T	adiabatic efficiency defined as the ratio of turbine work based on torque, primary weight flow, and speed measurements to ideal work based on inlet total temperature, and inlet and outlet total pressure both defined as sum of static pressure plus pressure corresponding to gas velocity
η_t	adiabatic efficiency defined as the ratio of turbine work based on measured inlet and exit total temperature to ideal work based on measured inlet total temperature and pressure and measured exit total pressure
θ_{cr}	squared ratio of critical velocity at turbine inlet temperature to critical velocity at standard sea level temperature
ν	ratio of blade speed to isentropic gas velocity based on inlet total temperature and pressure and exit static pressure $\frac{(ur)_m}{V'}$

Subscripts

0	station at stator inlet (all stations shown in Figure 4)
3	station at free-stream conditions between stator and rotor
5	station at outlet of rotor just downstream of trailing edge
6	station downstream from turbine
rel	relative condition
st	static condition
T	stagnation or total conditions
t	tip radius

Superscripts

'	ideal or isentropic
*	standard conditions

APPARATUS AND INSTRUMENTATION

The analyses and design of the turbine test rig and the blading are discussed in detail in reference 2. The turbine has a constant hub diameter of 21.0 inches and a constant tip diameter of 30.0 inches. The unit has 40 stator blades and 76 rotor blades. The overall design point equivalent characteristics are as follows:

- Equivalent specific work output, $\frac{E}{\theta_{cr}}$, Btu/lb 20.0
- Equivalent weight flow, $\frac{\dot{m}\sqrt{\theta_{cr}\epsilon}}{\delta_o}$, lb/sec 45.51
- Equivalent blade tip speed, $\frac{(ur)_t}{\sqrt{\theta_{cr}}}$, ft/sec 610.0

The design velocity diagrams are shown in Figure 2 and the tandem blade profiles are shown in Figure 3. The profile coordinates are included in reference 2. A photograph of the tandem blade rotor assembly is shown in Figure 1. The radial clearance between the blade tips and the turbine casing is approximately 0.030 inch.

The apparatus used in this investigation consisted of a single-stage cold air turbine test rig, suitable housings to provide uniform inlet flow conditions, and a dynamometer to absorb and measure the turbine power output. Airflow is supplied to the test rig by a separate air compressor facility. The air is supplied at approximately three-atmospheres pressure and a temperature of approximately 700°R. The facility air can be heated or cooled by heat exchangers. The facility air enters the plenum chamber through two diametrically opposed pipes. The air passes through the turbine blading and discharges into the facility exhaust system. The inlet pressure is controlled by the separate air compressor supply and/or by a throttle valve in the inlet supply line. The turbine expansion ratio is controlled by a throttle valve in the exhaust system duct. The turbine exhaust may either be discharged to the atmosphere or directed to an evacuator facility to provide below ambient exhaust conditions.

The turbine test rig instrumentation is described in detail in reference 2. The airflow is measured using a Bailey adjustable orifice which is calibrated with an ASME flow nozzle. The turbine power output is absorbed by two Dynamatic dry-gap eddy current brakes. The torque of each dynamometer is measured separately by a dual output strain gage load cell connected in tension to the dynamometer torque arm.

Measurements of total temperature, total pressure, and static pressure were made at stations 0 and 6 (Figure 4). Turbine inlet temperature was measured with 20 iron-constantan thermocouples arranged five to a rake. The sensing

elements were located on centers of equal annular areas, and the rakes were spaced 90 degrees apart. Four Kiel type total pressure probes, also located at the inlet, were used to establish the desired inlet total pressure. Four static pressure taps on both the inner and outer walls were located around the annulus at stations 0, 5, and 6.

The turbine exit measuring station (station 6, Figure 4) was instrumented with five combination total pressure, total temperature, self-aligning flow angle probes. The sensing elements of the five combination probes were located at the center of five equal annular areas.

Stator outlet (station 3, Figure 4) static pressures were measured by four static pressure taps located 90 degrees apart on both the inner and outer walls immediately downstream of the stator blade trailing edge. Each tap was centrally located on the projected stator flow passage.

Two surveys were made approximately 1/8-inch downstream of the rotor blade trailing edge (station 5, Figure 4). Total pressure, total temperature, and flow angle were measured at five radii from hub to tip for a circumferential arc of 22 degrees. The measurements were taken concurrently with a single combination probe. The second survey was made with a hot-film anemometer probe consisting of a radially mounted 0.002-inch diameter quartz rod with a very thin platinum plating over the quartz. The maximum frequency response of the sensing element is approximately 40,000 cycles per second. This probe was installed in the same mounting pad as the pressure, temperature, flow angle probe and was positioned circumferentially to avoid the stator wakes determined from the total pressure survey of an earlier test (reference 1).

CALCULATION PROCEDURE

OVERALL TURBINE PERFORMANCE

The turbine performance was rated on the basis of two expansion ratios defined as (1) the ratio of the inlet total pressure to rotor discharge static pressure and (2) the ratio of inlet total pressure and rotor exit total pressure. The inlet total pressure at station 0 was calculated from continuity using the average of the 20 measured total temperatures, the average of the hub and tip static pressures, the mass flow rate, and the inlet annulus area. The flow was assumed to be axial. The exit total pressure at station 6 was also calculated from continuity using the mass flow rate, the annulus area, the average of the hub and tip static pressures, the average flow angle, and the total temperature. The total temperature was calculated from the enthalpy drop which in turn was based on the measured airflow, torque, and speed.

The efficiencies were calculated as a ratio of the actual enthalpy drop as obtained from torque, mass flow rate, and rotor speed measurements to the ideal enthalpy drop as obtained from the inlet total temperature and the associated calculated expansion ratio.

ROTOR EXIT SURVEY

The performance of the turbine as described by a rotor exit survey at the design point condition is based on measured expansion ratio, inlet temperature, and exit temperature. The measured expansion ratio is based on the average total pressure indicated by the four inlet Kiel probes and the exit total pressure measured by the survey probe. The inlet total temperature is the average temperature of the 20 inlet thermocouples; the exit total temperature is measured by the thermocouple on the survey probe. These thermocouples were corrected for Mach number based on a linear variation of hub and tip static pressure and the measured total pressure. The isentropic work of the turbine is based on the measured inlet temperature and measured total pressure ratio. The actual work is the difference of the enthalpies associated with the measured inlet and exit temperatures. The efficiency at each station in the survey is the ratio of the actual work to the isentropic work.

The measured absolute flow angle and an assumed linear variation of static pressure from hub to tip were used to determine the velocity diagrams at the rotor exit. The stator exit whirl was calculated as a function of circumferential position at each radial depth from the work based on measured temperatures, the blade speed, and the rotor exit whirl. These stator exit whirls and rotor exit relative angles were then used to determine the rotor relative total pressure loss from the hot-wire survey.

HOT-WIRE SURVEY

The procedure followed for the reduction of the basic hot-wire electronic signals is described in reference 3. This data reduction procedure produces the variation of absolute gas velocity and total temperature with blade passage circumferential position at a given radial-circumferential position. The reduction of these variables to a loss of rotor relative total pressure is described in reference 4. The rotor exit relative discharge angle and the stator exit whirl velocity were determined from the rotor exit survey calculation rather than using the design value. The stator exit absolute total pressure was based on the measurement of the stator loss survey (reference 1).

EXPERIMENTAL RESULTS

TURBINE OVERALL PERFORMANCE

The overall performance of the turbine with the tandem blade rotor assembly is shown in Figure 5 as a composite map. This map presents the equivalent shaft work, E/θ_{cr}, as a function of the equivalent flow-speed parameter, $\frac{\dot{m}N\epsilon}{60\,\delta_o}$, for lines of constant total-to-total expansion ratio, P_{T0}/P_{T6}, and equivalent rotor speed, $N/\sqrt{\theta_{cr}}$. Contours of constant total efficiency, η_T, are also included. The design equivalent work and speed are indicated by point A on the map, while the design equivalent work and flow-speed parameter are shown by point B. Comparison of the flow-speed parameter of these two points indicates the turbine flow capacity was approximately five percent greater than design. This is comparable to the flow capacity of the turbine with the plain blade installed. The excess flow in both of these tests is because of the increase in stator area that resulted from a welding operation of the stator (reference 1).

The variation of equivalent torque, $\Gamma\epsilon/\delta_o$, and equivalent weight flow, $\frac{\dot{m}\sqrt{\theta_{cr}}\,\epsilon}{\delta_o}$, with overall total-to-total expansion ratio and equivalent speed are shown in Figures 6 and 7, respectively. The torque characteristic of Figure 6 indicates that limiting loading had not yet been achieved at the high expansion ratio condition. At the 100 and 110 percent equivalent speeds, expansion ratios of approximately 2.3 were not exceeded because of blade dynamic stress. At the lower rotor speeds, expansion ratios were limited to a maximum of about 2.5 for the same reason. The equivalent flow characteristics of Figure 7 indicate the turbine is choked at the design expansion ratio of 2.1 and above. Also, the range of equivalent speeds investigated had only minor influence on the turbine flow characteristics.

A plot of total-to-total efficiency is presented in Figure 8 as a function of blade-jet speed ratio. A single curve was drawn through the bulk of the data; however, at the lower values of blade-jet speed ratio, the lower speed data indicate a distinct curve having a change in slope for each speed. Additional data at high pressure ratios (low blade-jet speed ratios) are required to define the shape of the curves in this region. At the design blade-jet speed ratio of 0.438, the efficiency was 87.7 percent, reaching a maximum of about 90.5 percent at a blade-jet speed ratio of 0.55. The level of efficiency is significant because the rotor performance was achieved with negative hub reaction.

An insight into the degree of negative reaction achieved is shown in Figure 9 which shows the hub and tip static pressure variation through the turbine as a function of overall total-to-total expansion ratio. At the design expansion ratio

of 2.1, the rotor hub inlet and exit static pressure ratios were 0.35 and 0.403 compared with the design values of 0.36 and 0.41. This indicates a slightly greater degree of negative hub reaction than design. Also, the rotor inlet tip static pressure ratio of 0.528 is lower than the design value of 0.59, indicating that the overall rotor system is operating at a lower level of reaction than design. This low level of reaction combined with the high efficiency is also significant because of the effect of the larger than design stator throat area. The increased stator area tends toward positive rotor reaction and is being offset by the increased effective flow area of the tandem blade.

TURBINE LOCAL EFFICIENCY SURVEY

Circumferential traverses of a combination total pressure, temperature, and yaw angle probe were made at constant radii to map the flow characteristics at the rotor trailing edge. These surveys yield the circumferential variations of temperature ratio, $(T_{T0} - T_{T5})/T_{T0}$, total pressure ratio, P_{T0}/P_{T5}, blade exit absolute flow angle, and local efficiency. Typical examples of these survey traces are shown in Figures 10 through 13. From these surveys, a contour map of turbine efficiency was constructed based on the locally measured total-to-total expansion ratio. This contour map is shown in Figure 14. The major portion of the sector surveyed had efficiencies ranging from 80 percent just above the hub to about 96 percent in a region between the mean and tip sections, with the lower efficiencies generally occurring at the blade hub. These large areas of lower efficiency in the hub region together with the stator survey presented in reference 1, indicate greater rotor losses in this area. These losses are substantiated in the following subsection.

ROTOR EXIT HOT-WIRE SURVEY

A hot-wire anemometer survey was conducted at the rotor trailing edge. The turbine exit total pressure survey was used to define the radial-circumferential path of the hot-wire probe to avoid the stator wakes. The results of this survey are presented as contours of rotor relative total pressure ratio, $P_{T5\ rel}/P_{T3\ rel}$, in Figure 15. The absolute magnitude of the rotor relative pressure ratio is recognized to be high in level. The specific cause for this error is not known. However, the data are presented to illustrate the relative magnitude, shape, and location of the loss areas.

The wakes of the secondary and primary airfoils are shown in Figure 15, along with the pressure and suction sides of the blade wake. The pressure side boundary layer appears to be thicker than the suction side. There is no apparent explanation for this characteristic. The primary airfoil wake appears smaller than the secondary blade wake; however, this could be the result of mixing. The hub section has large areas of loss indicating probable separation.

COMPARISON OF PERFORMANCE OF TANDEM BLADE WITH THAT OF PLAIN BLADE

A comparison of the overall performance map of the tandem blade shown in Figure 5 can be made with the overall performance map of the plain blade presented in Figure 16. Both turbines exhibited approximately the same design point overall efficiency of 88 percent; however, the two turbines performed differently over other regions of the map. At low rotor speeds and higher expansion ratios (low values of blade-jet speed ratio), the plain blade turbine had a higher efficiency and, therefore, a higher specific work output than the tandem blade turbine. At a pressure ratio of 2.1 and 80 percent design speed, the plain blade specific work was 20.1 Btu/lb compared to 19.5 Btu/lb for the tandem blade. At higher rotor speeds and, therefore, higher values of blade-jet speed ratio, the tandem blade turbine performance was slightly better than the plain blade turbine. At the same expansion ratio but at 110 percent design speed, the plain blade specific work was 21 Btu/lb compared to 21.3 Btu/lb for the tandem blade.

The equivalent flow characteristics of the tandem blade turbine shown in Figure 7 can be compared with those of the plain blade turbine shown in Figure 17. Both turbines are choked at the design expansion ratio of 2.1 and above. Rotor equivalent speed effects are small for both turbines, but the tandem blade shows speed to have more influence on equivalent flow in the choked flow region than the plain blade.

A very significant difference in the performance characteristics of the two turbines is shown by comparing the static pressure distribution through the turbine with the overall expansion ratio. This distribution at 100 percent equivalent speed is shown for the tandem blade in Figure 9 and for the plain blade in Figure 18. Both turbines have approximately the same static pressure variation with expansion ratio at the stator inlet (station 0) and rotor exit (station 6). However, the stator outlet (station 3) hub and tip static pressures are lower with the tandem blades installed than with the plain blades installed. This characteristic is present over the entire range of expansion ratios covered, showing that the tandem blade was operating with a lower degree of rotor reaction than the plain blade. The rotor hub reaction of the tandem blade differs very little from the plain blade up to an expansion ratio of 1.9, but is significantly different at higher expansion ratios. Beyond an expansion ratio of 2.13, the plain blade reaction was positive, while the tandem blade hub reaction was negative over the entire range of expansion ratios investigated. This results in the tandem blade turbine operating at higher stator exit absolute and rotor inlet relative velocities than that encountered in the plain blade turbine test.

Another interesting difference in the two turbines is shown by the presence of choking in the plain blade rotor and the absence of choking in the tandem rotor blade. The evidence of plain rotor choking is shown in Figure 18 at an expansion ratio of 2.1. At this expansion ratio, the stator exit static pressure remains

constant as overall expansion ratio is increased, indicating a choked condition somewhere between the stator exit and the rotor downstream measuring station. Measurements of the plain blade surface static pressures described in reference 1 indicate choking in the blade passage at expansion ratios greater than 2.13. Both rotors have the same measured blade channel area at the rotor trailing edge. Therefore, the plain blade must have a limiting flow area at some position inside the blade channel and/or higher rotor losses to reduce the effective rotor flow area.

A comparison of the tandem blade local efficiency survey shown in Figure 14 can be made with the plain blade survey shown in Figure 19. These contour plots were constructed from the circumferential variation of efficiency at a constant depth as shown in Figure 13. By graphically integrating these traces at each radial depth, a plot of the average circumferential efficiency at station 5 as a function of radius can be constructed. The radial variation in efficiency for both the plain blade and tandem blade is shown in Figure 20. Integration of this plot results in an overall turbine efficiency at station 5 of 87.1 percent for the plain blade and 89.3 percent for the tandem blade. Both units exhibited approximately the same efficiency at station 6. The larger change in efficiency from station 5 to station 6 for the tandem blade may be the result of increased mixing losses downstream of the tandem blade. The presence of two wakes per blade is shown in the hot-wire survey and is possibly causing more mixing losses downstream of the trailing edge for the tandem blade. Another possible cause for the efficiency variation is the inability to mass average the efficiency variations both radially and circumferentially.

SUMMARY OF RESULTS

The overall performance of a single-stage turbine with a tandem rotor blade was investigated over a range of equivalent speeds and expansion ratios and compared with the performance of a plain rotor blade. Both rotor blade configurations were designed to the same velocity diagrams which had negative rotor hub reaction. The following results were obtained.

1. The total efficiency of the turbine with the tandem blade installed was 87.6 percent at the design speed and expansion ratio. This is comparable to the plain blade efficiency of 88.4 percent.

2. At corresponding expansion ratios, the tandem blade turbine had somewhat higher efficiency at speeds above design speed than the plain blade turbine but lower efficiency at reduced speed.

3. The equivalent flow characteristics of both turbines were essentially the same. At the design and higher expansion ratios, both turbines were choked for all rotor speeds tested.

4. The general level of tandem rotor reaction was slightly lower than the plain blade for pressure ratios up to 1.9 and was significantly lower for higher expansion ratios.

5. Static pressures at the tandem rotor hub indicated negative reaction for the entire expansion ratio range covered. At design speed and expansion ratio, the static pressure rise across the hub was slightly greater than design.

6. Interstage static pressures also showed that the tandem rotor was not choked at the highest expansion ratio tested (2.3). The plain blade was choked at the design expansion ratio of 2.1. Since the measured blade channel area at the rotor trailing edge was the same for both rotors, the reduced effective flow area of the plain blade is the result of higher rotor losses, and/or the limiting flow area of the blade is located inside the blade channel.

7. A survey taken at the rotor trailing edge showed that the tandem blade turbine had slightly higher efficiency than the plain blade turbine. The slightly lower overall efficiency of the tandem blade turbine may be caused by higher mixing losses downstream of the survey plane.

REFERENCES

1. Lueders, H. G. Experimental Investigation of Advanced Concepts to Increase Turbine Blade Loading. Volume II. Performance Evaluation of Plain Rotor Blade. Allison Division, General Motors. EDR 4909. 21 March 1968.

2. Lueders, H. G. Experimental Investigation of Advanced Concepts to Increase Turbine Blade Loading. Volume I. Analysis and Design. NASA. CR-735. June 1967.

3. Baldwin, L. V., Sandborn, V. A., and Laurence, J. C. "Heat Transfer from Transverse and Yawed Cylinders in Continum, Slip, and Free Molecular Air Flows." ASME Journal of Heat Transfer. May 1960.

4. Kofskey, M. G. and Allen, H. W. Investigation of a 0.6 Hub-Tip Radius-Ratio Transonic Turbine Designed for Secondary Flow Study. IV. Rotor Loss Patterns as Determined by Hot-Wire Anemometers with Rotor Operating in a Circumferentially Uniform Inlet Flow Field. NACA. RME58B27. May 1958.

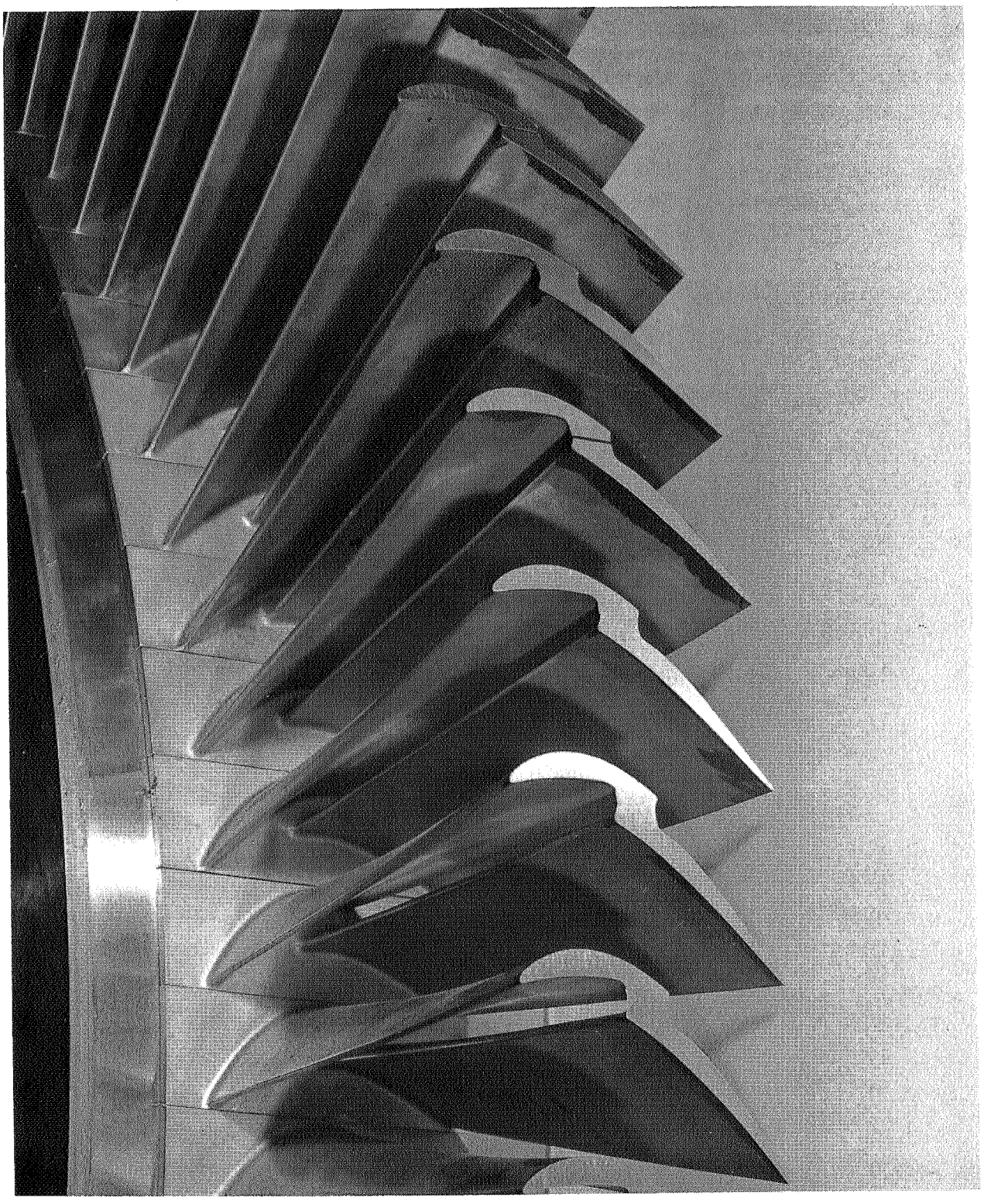

Figure 1. Tandem rotor blade assembly.

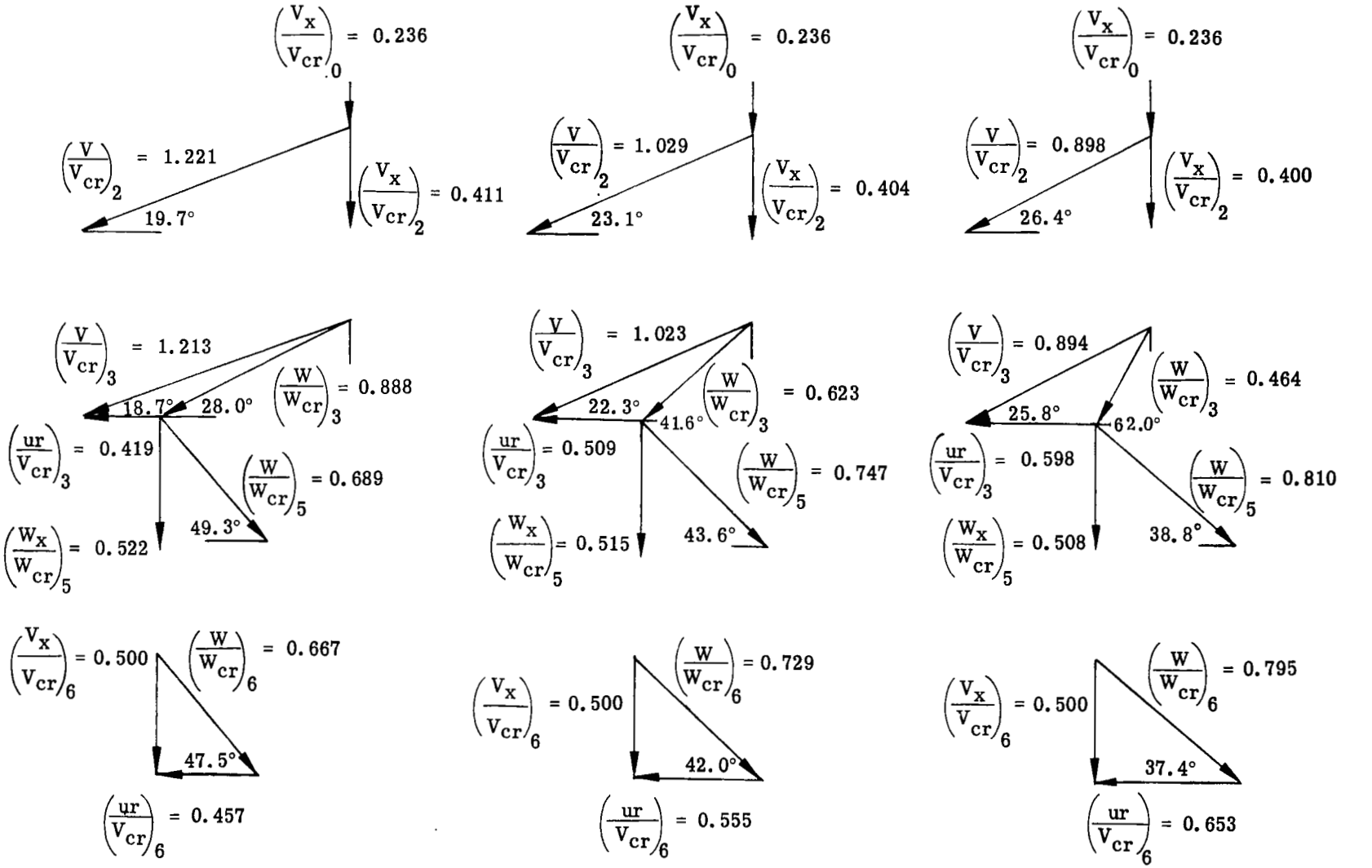

Figure 2. Design velocity triangles.

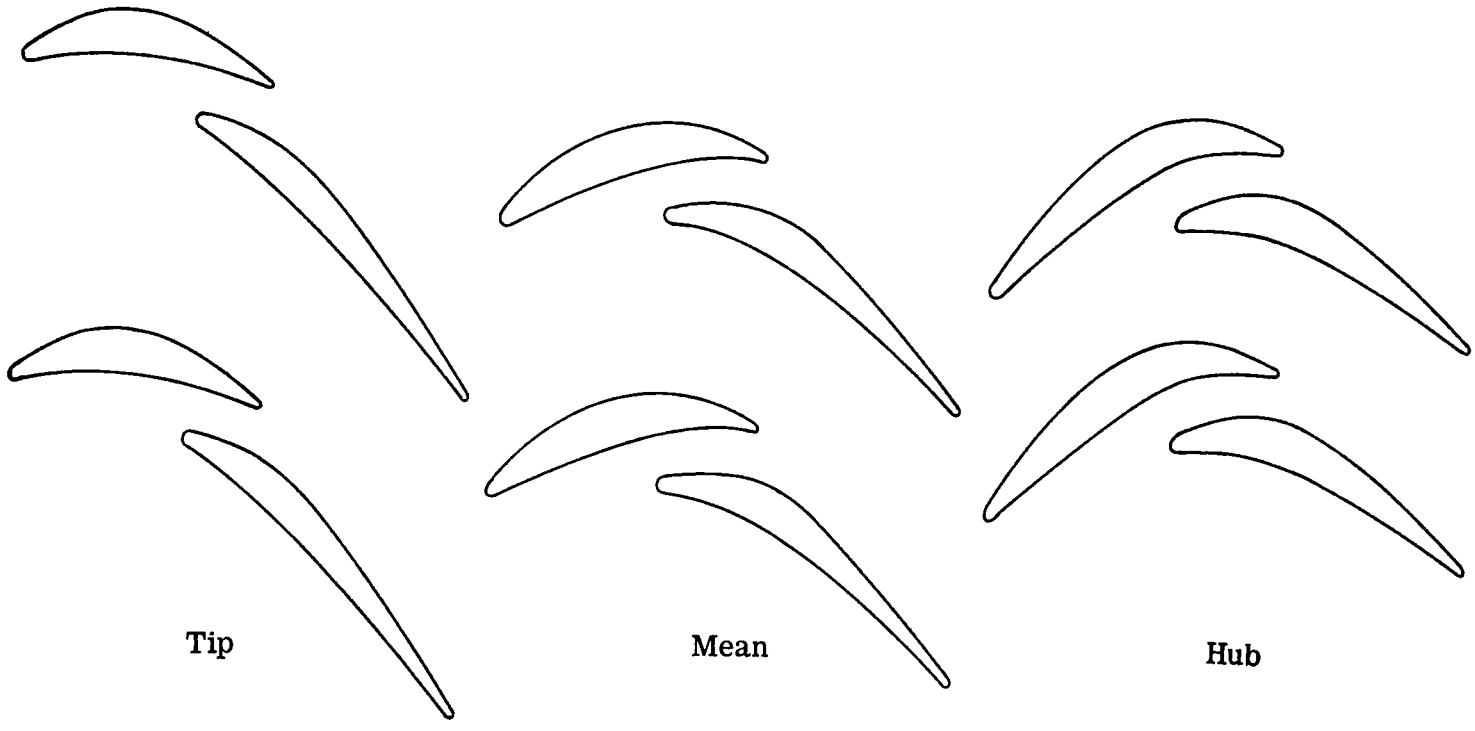

Figure 3. Tandem rotor blade profiles and channels.

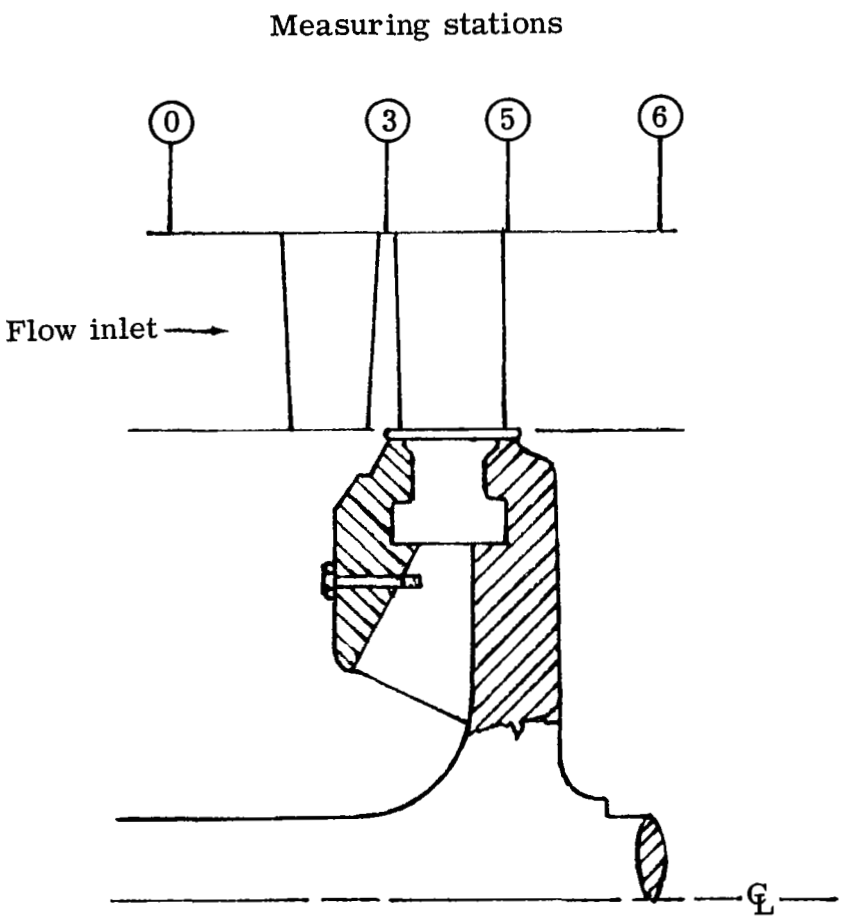

Figure 4. Schematic of flow path and station nomenclature.

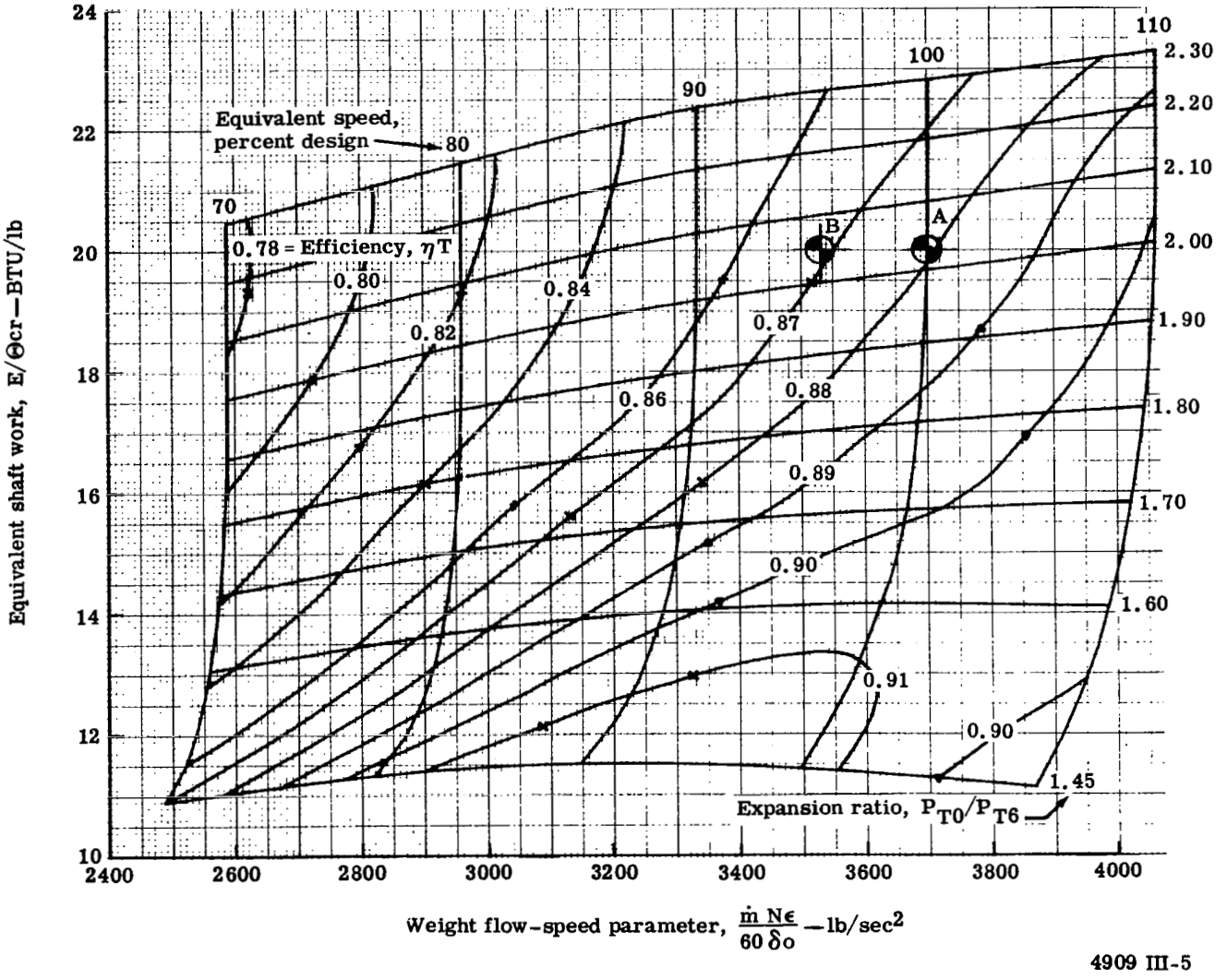

Figure 5. Overall performance of tandem rotor blade turbine.

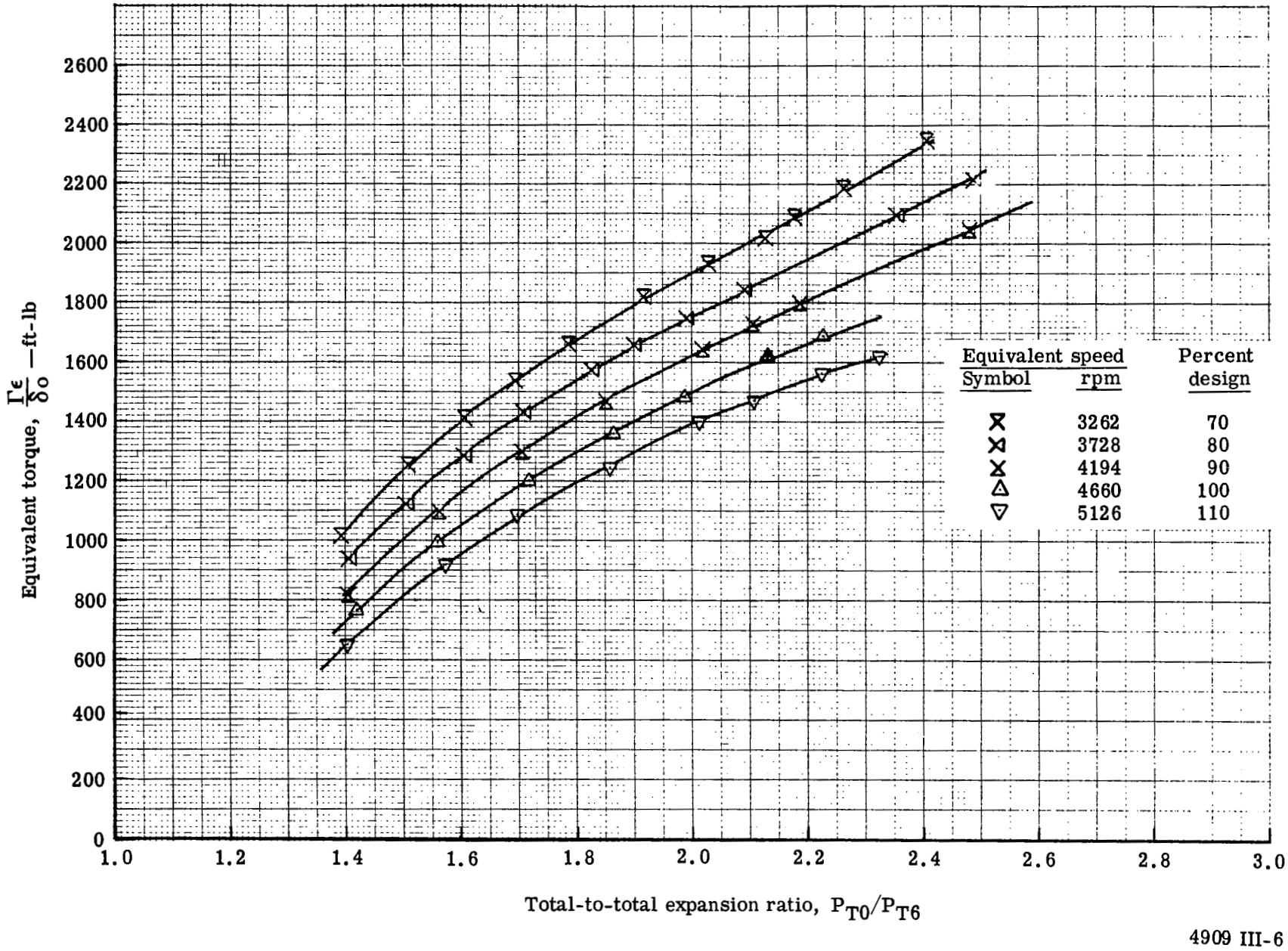

Figure 6. Variation of equivalent torque with expansion ratio for lines of constant equivalent speed.

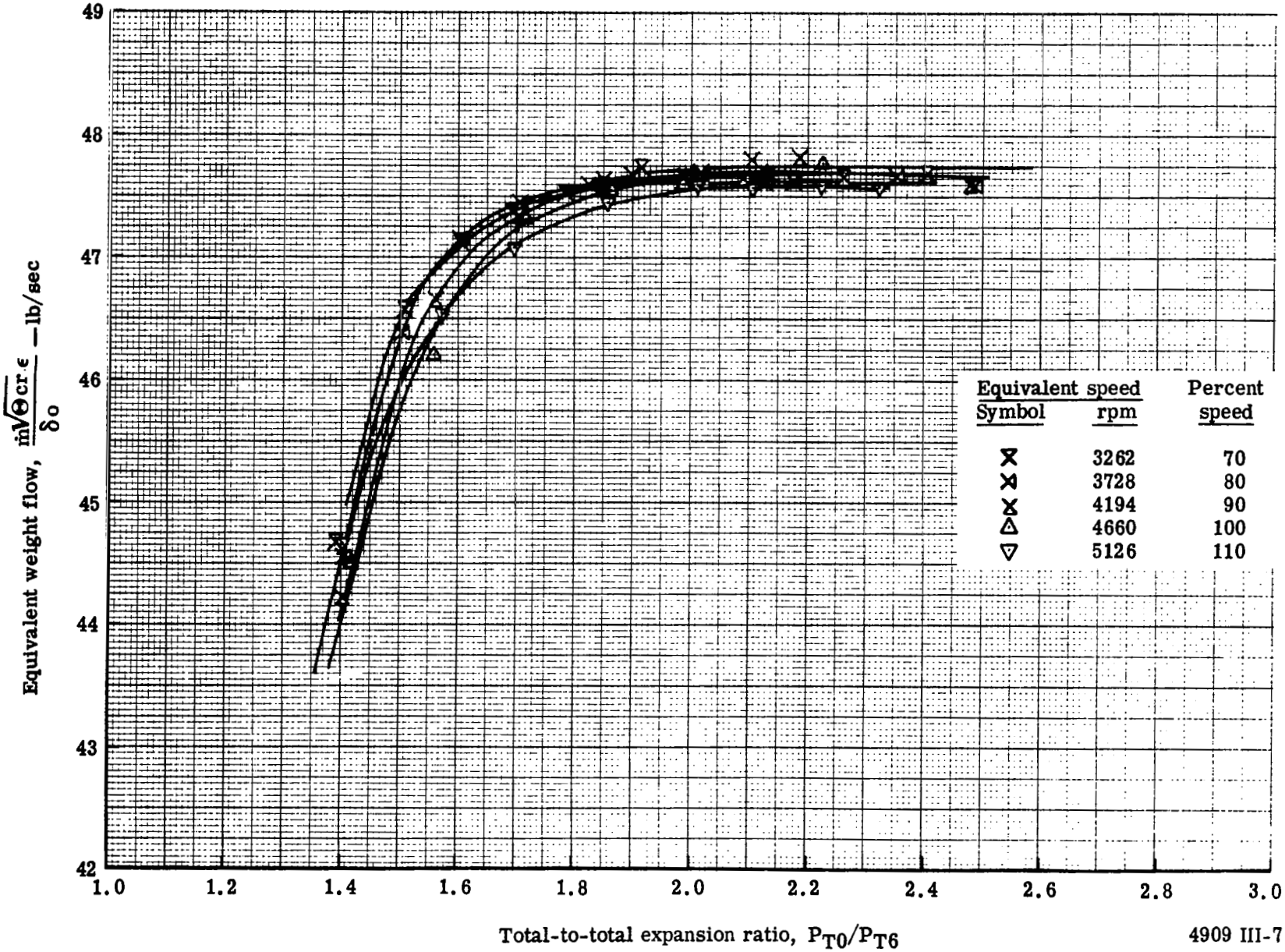

Figure 7. Variation of equivalent weight flow with expansion ratio for lines of constant equivalent speed.

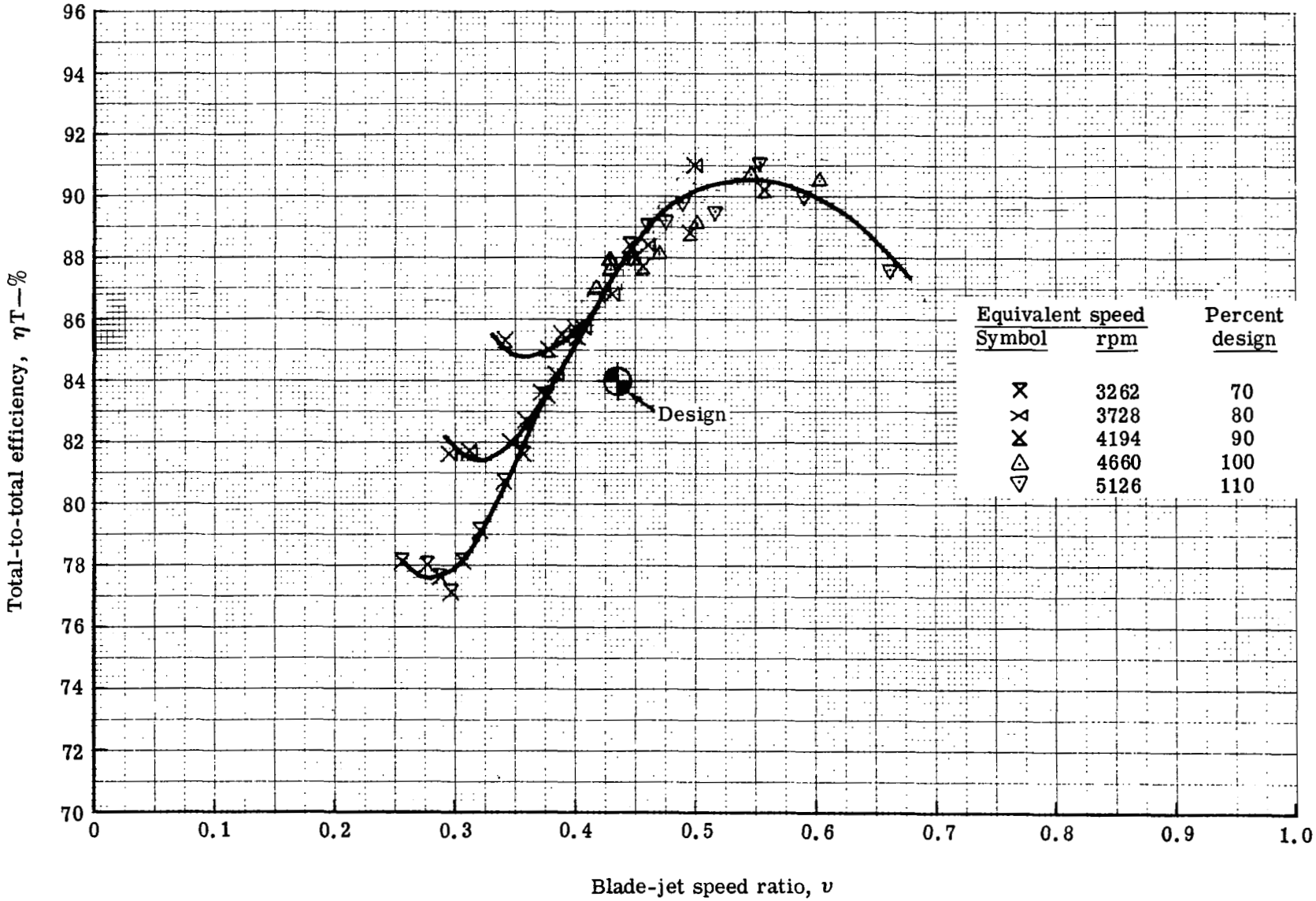

Figure 8. Variation of efficiency with blade jet-speed ratio for lines of constant equivalent speed.

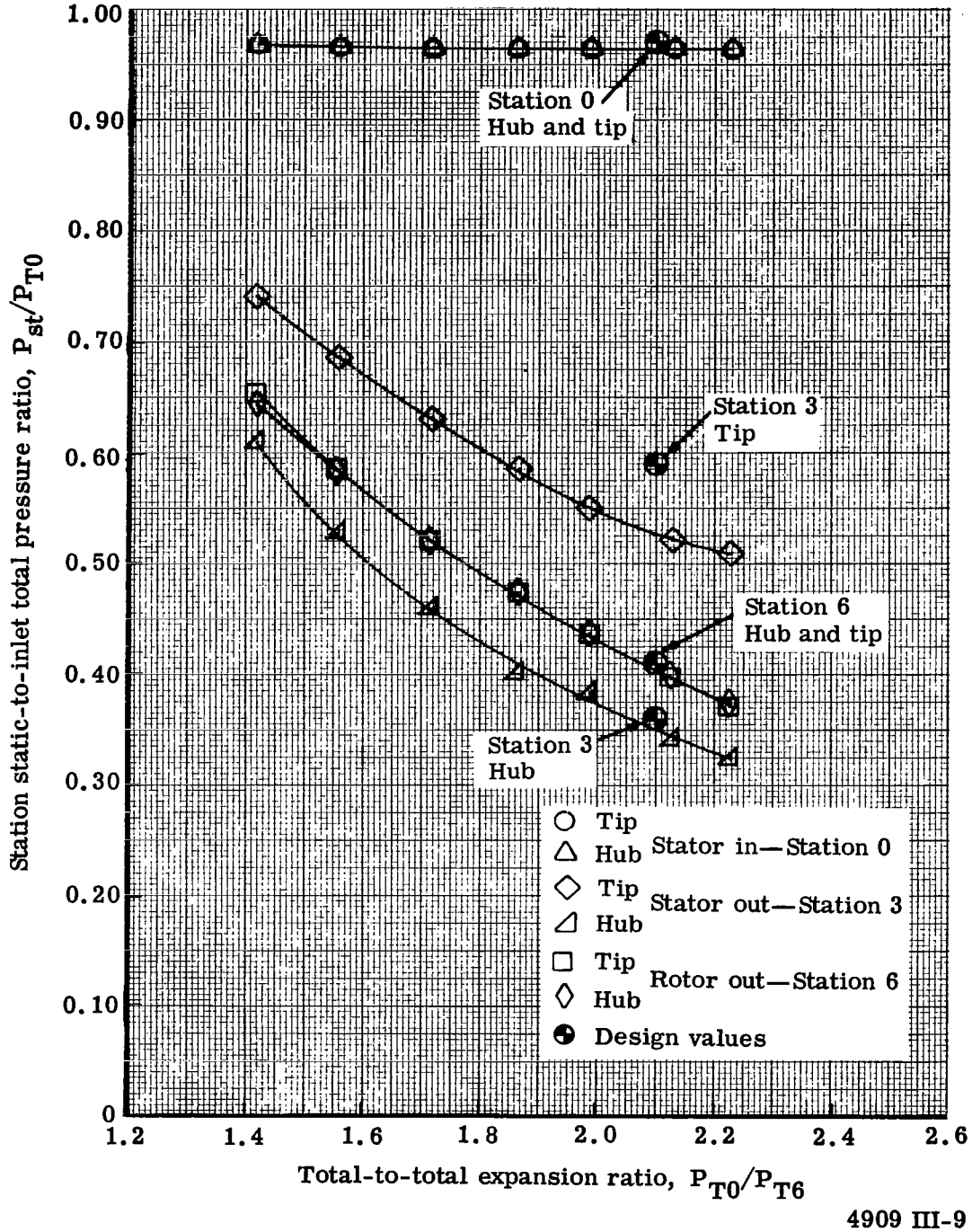

Figure 9. Variation of station hub and tip static pressure with turbine expansion ratio at design equivalent speed.

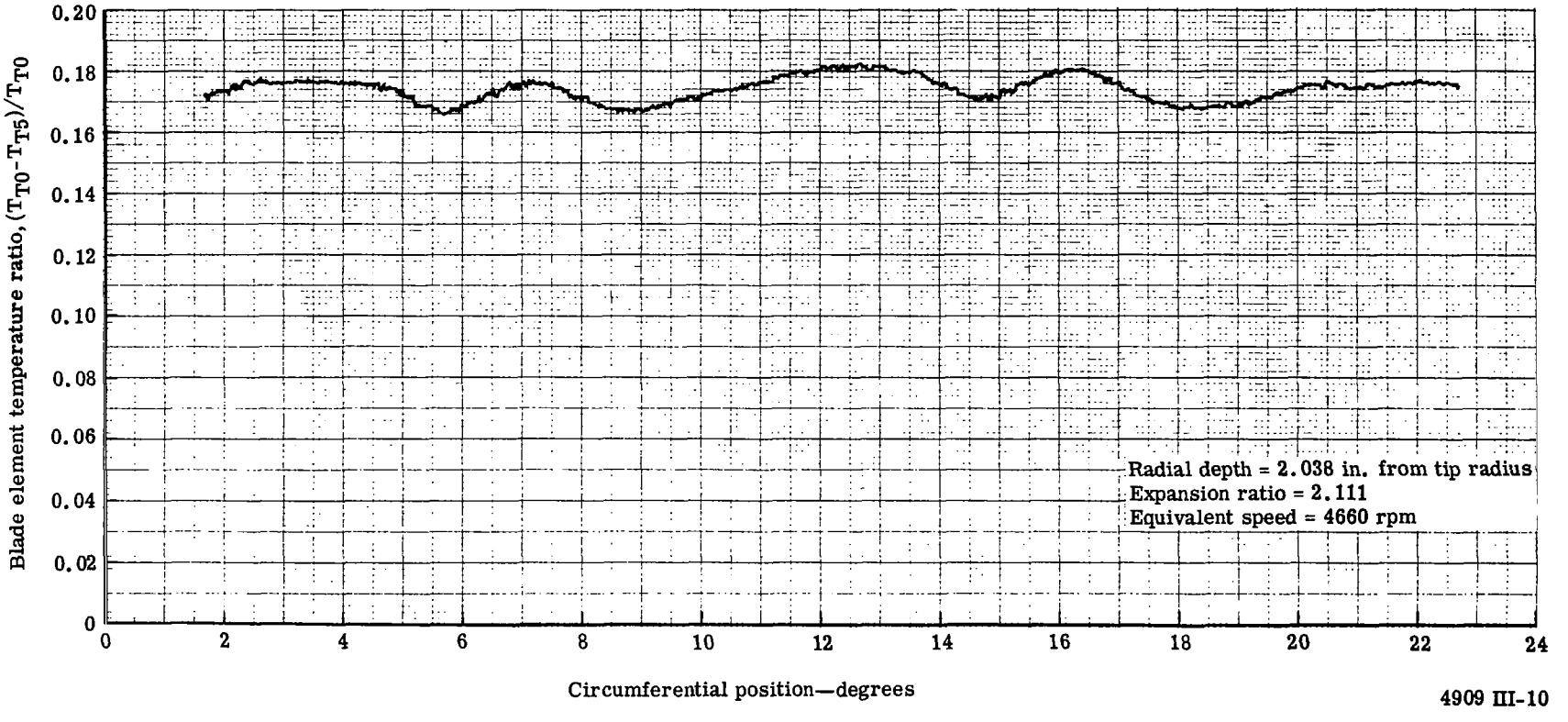

Figure 10. Circumferential variation of blade element temperature ratio recorded during rotor exit survey.

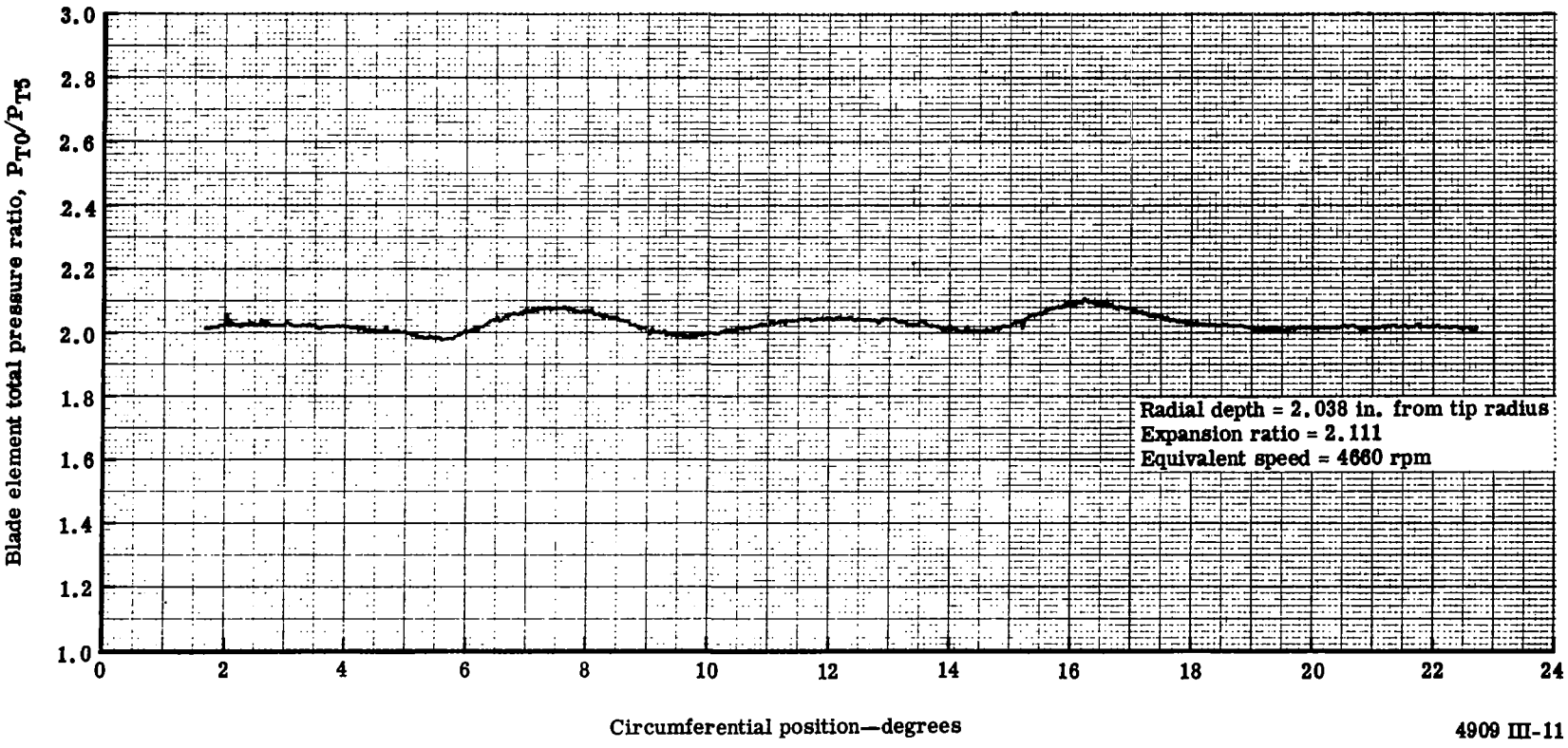

Figure 11. Circumferential variation of blade element total pressure ratio recorded during rotor exit survey.

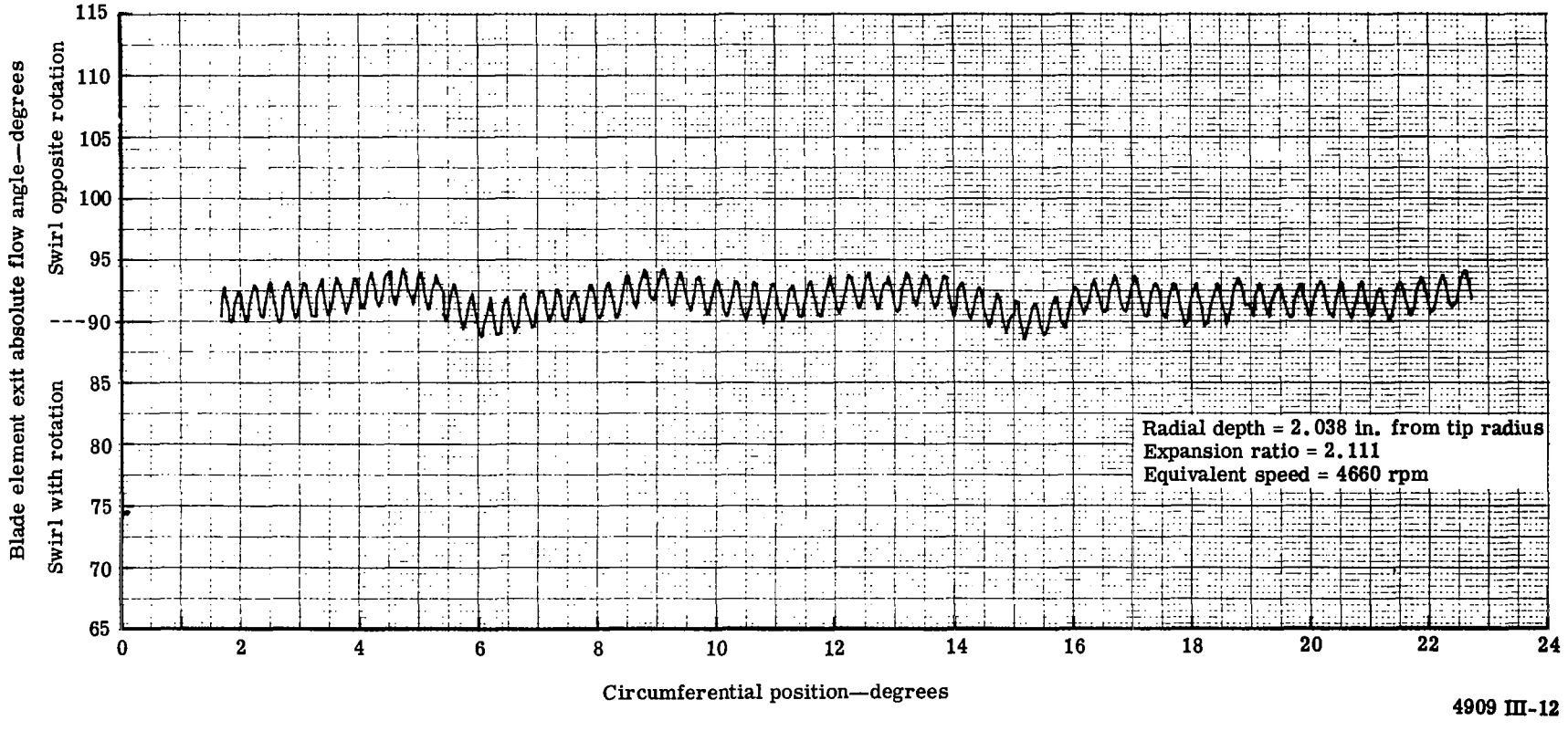

Figure 12. Circumferential variation of blade element exit absolute flow angle recorded during rotor exit survey.

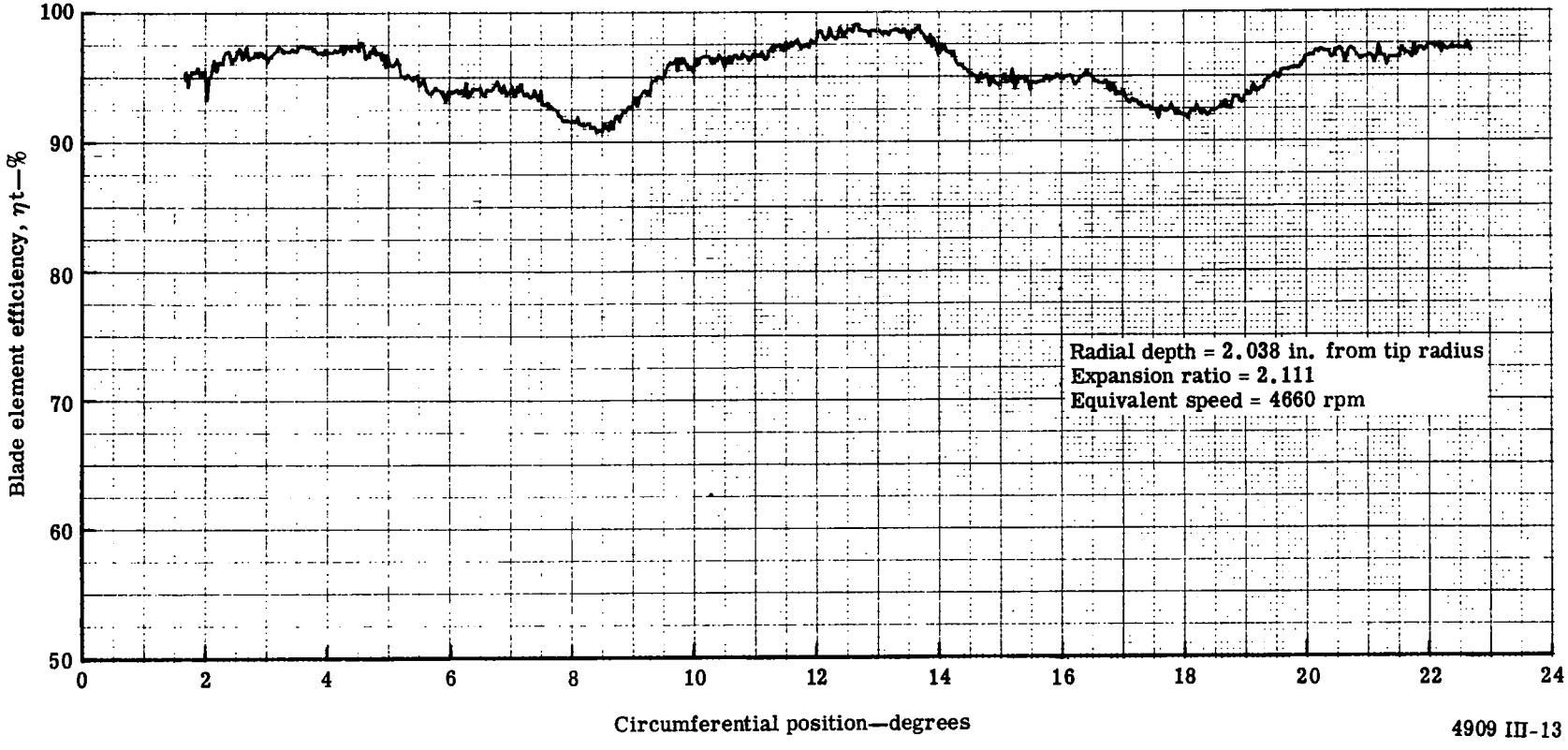

Figure 13. Circumferential variation of blade element total efficiency calculated from rotor exit survey data.

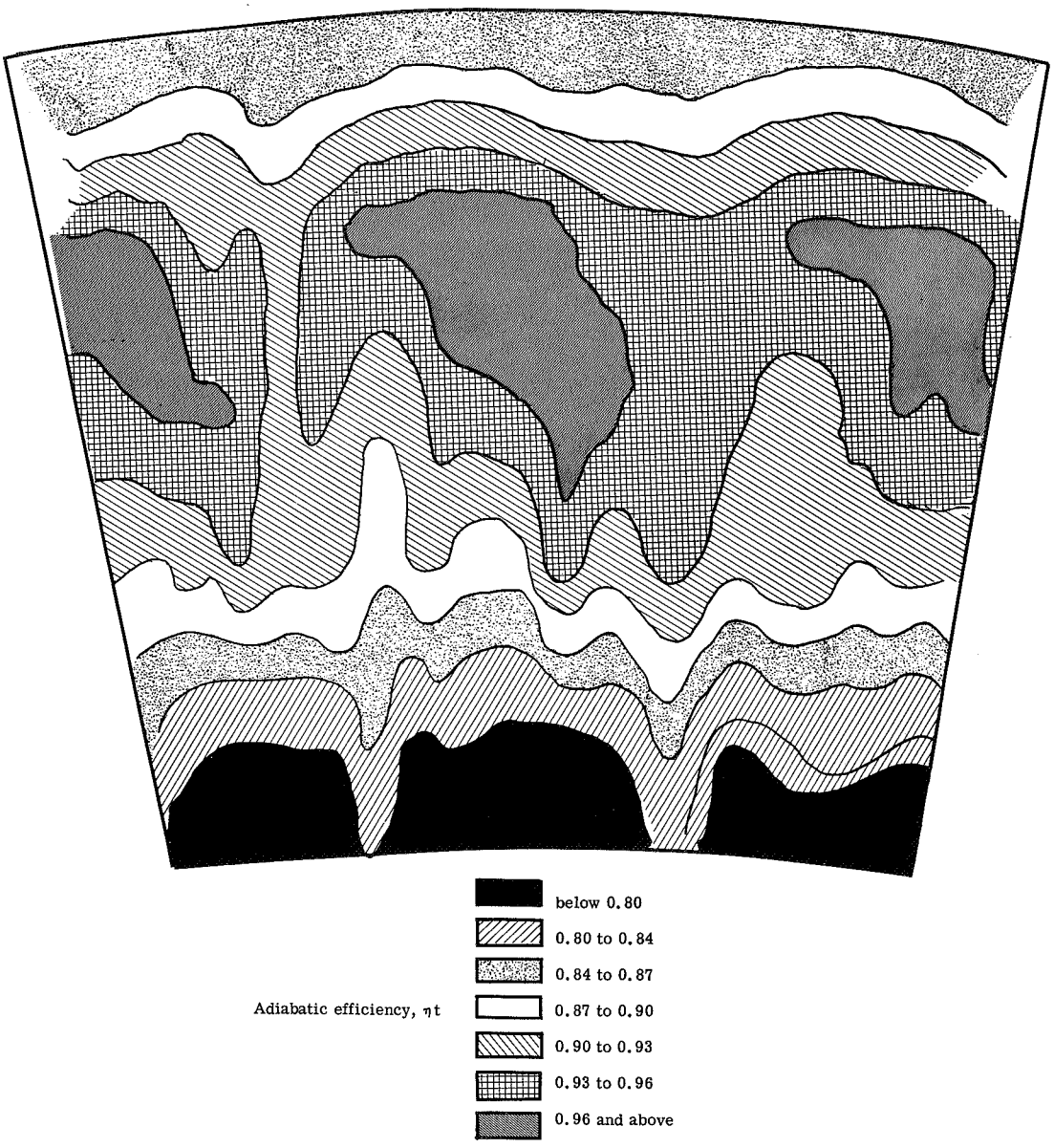

Figure 14. Turbine stage efficiency contours.

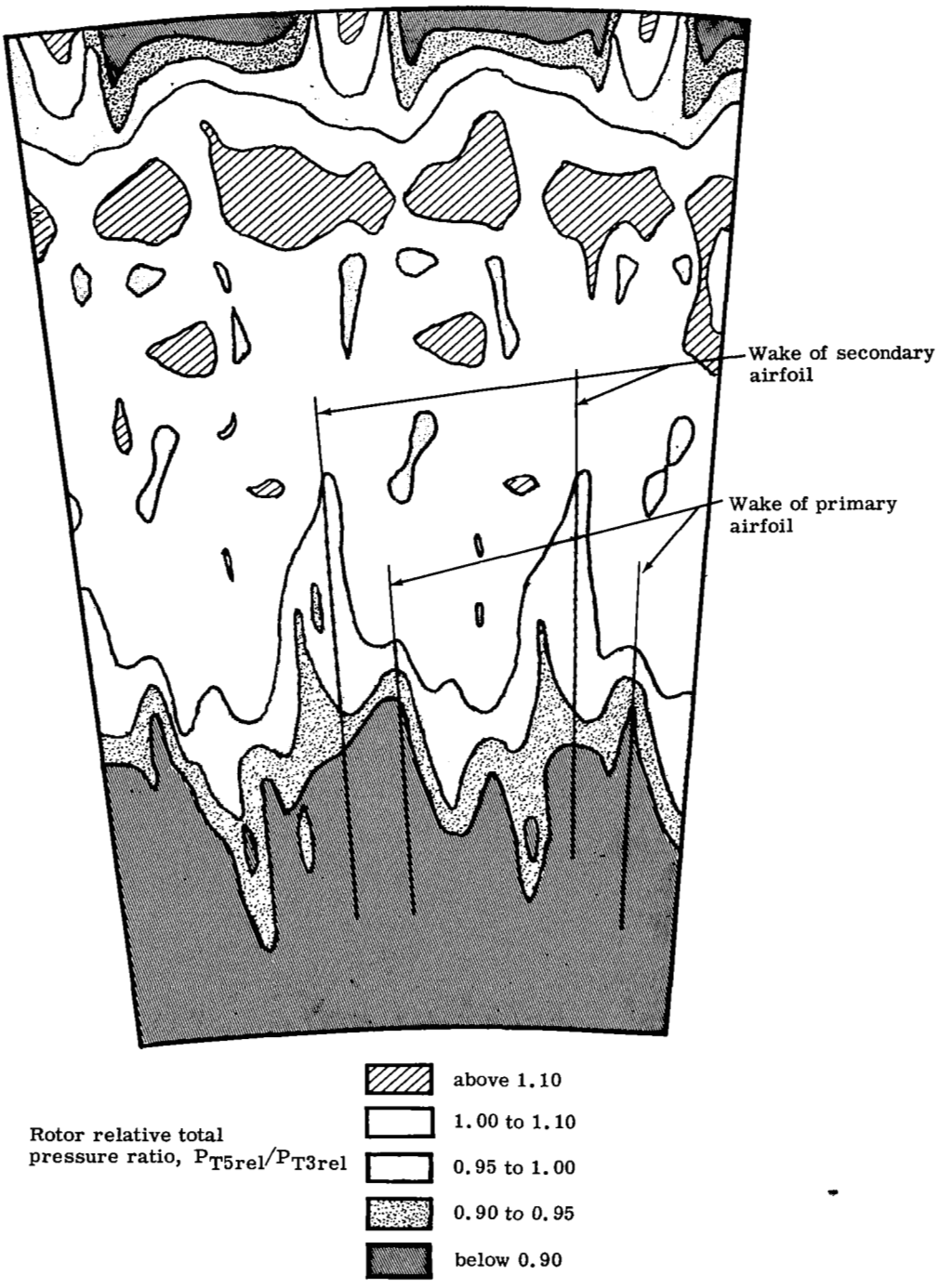

Figure 15. Rotor relative total pressure contours as determined from hot-wire survey.

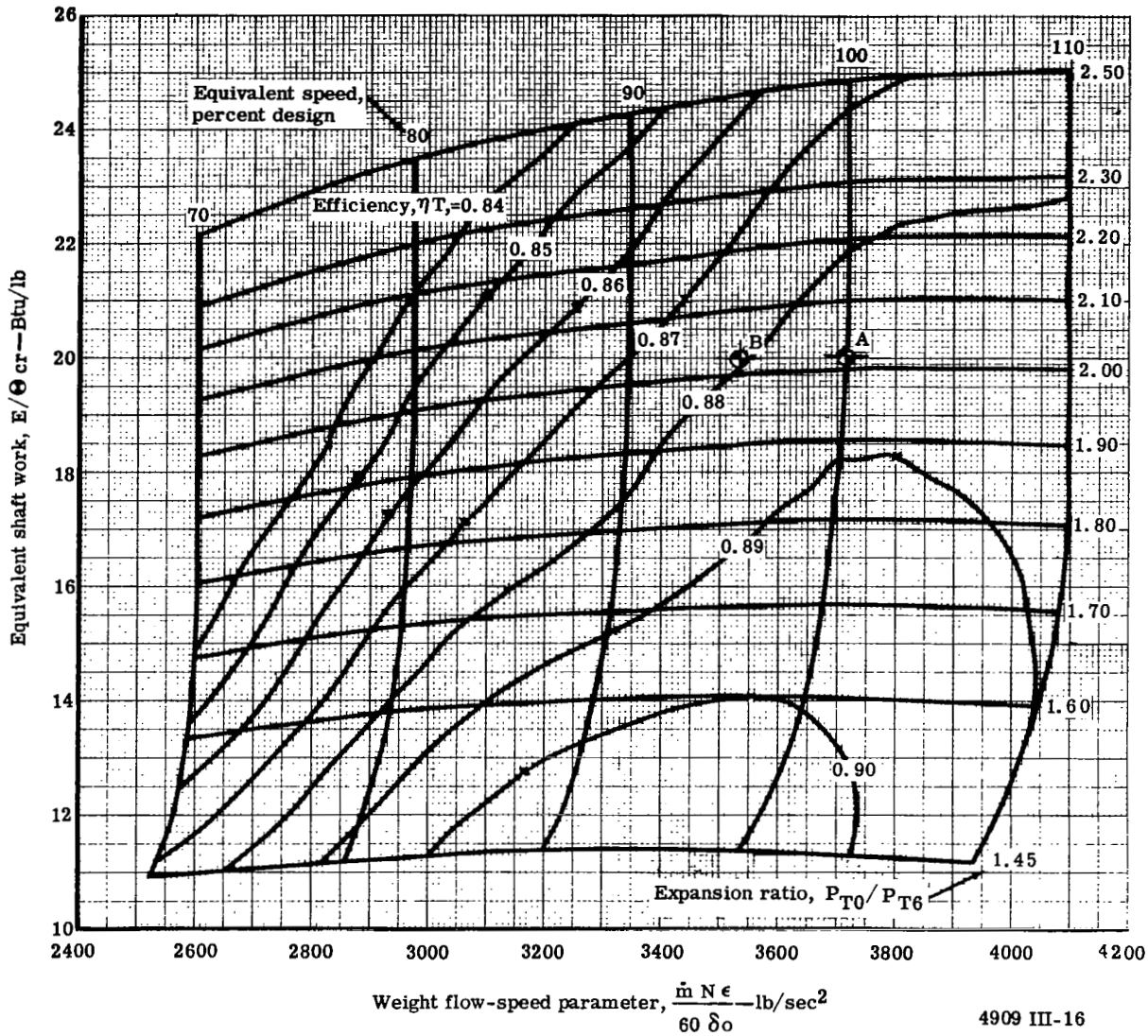

Figure 16. Overall performance of plain rotor blade turbine.

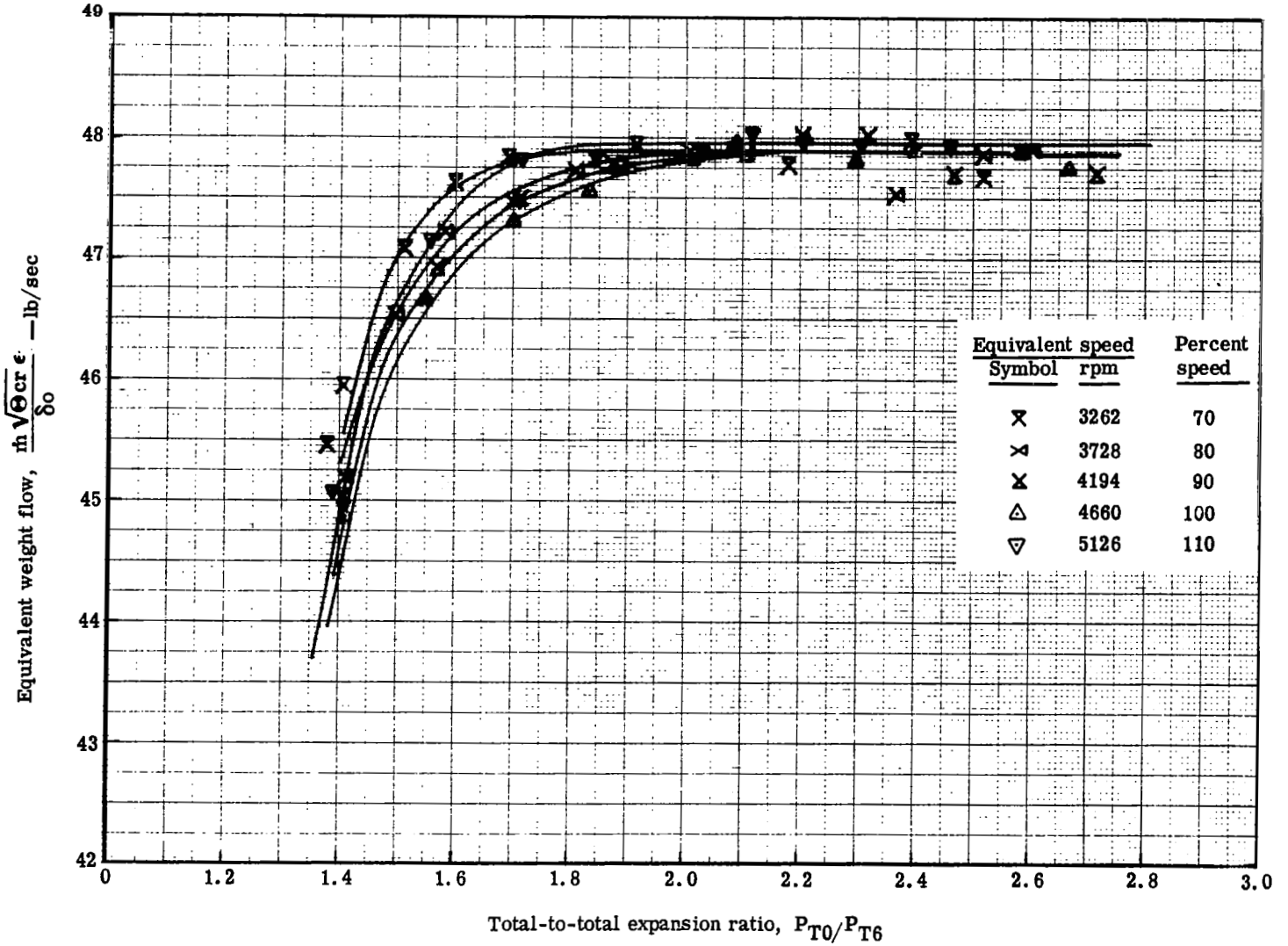

Figure 17. Variation of equivalent weight flow with expansion ratio for lines of constant equivalent speed for plain blade.

4909 III-17

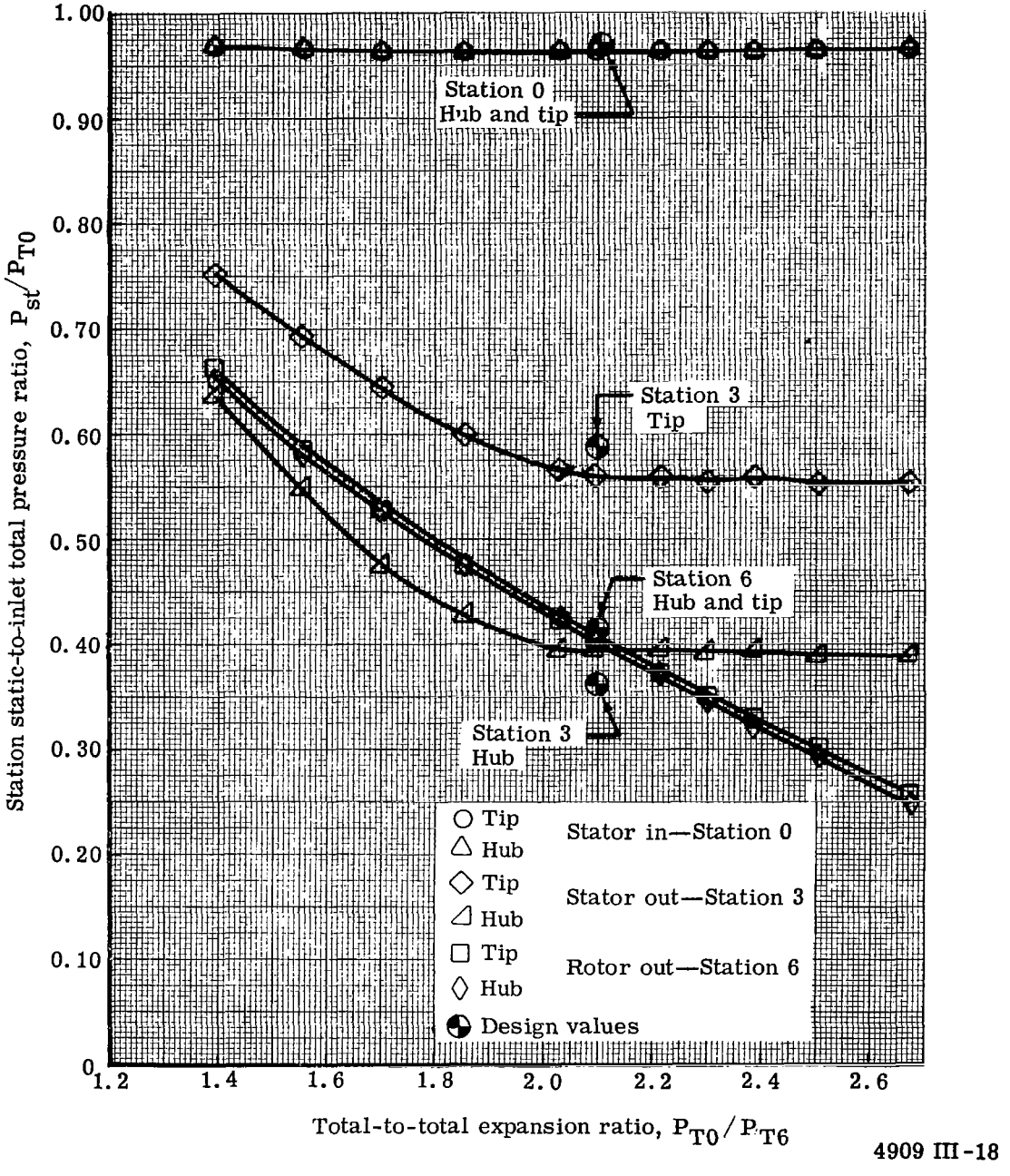

Figure 18. Variation of station hub and tip static pressure with turbine expansion ratio at design equivalent speed for plain rotor blade.

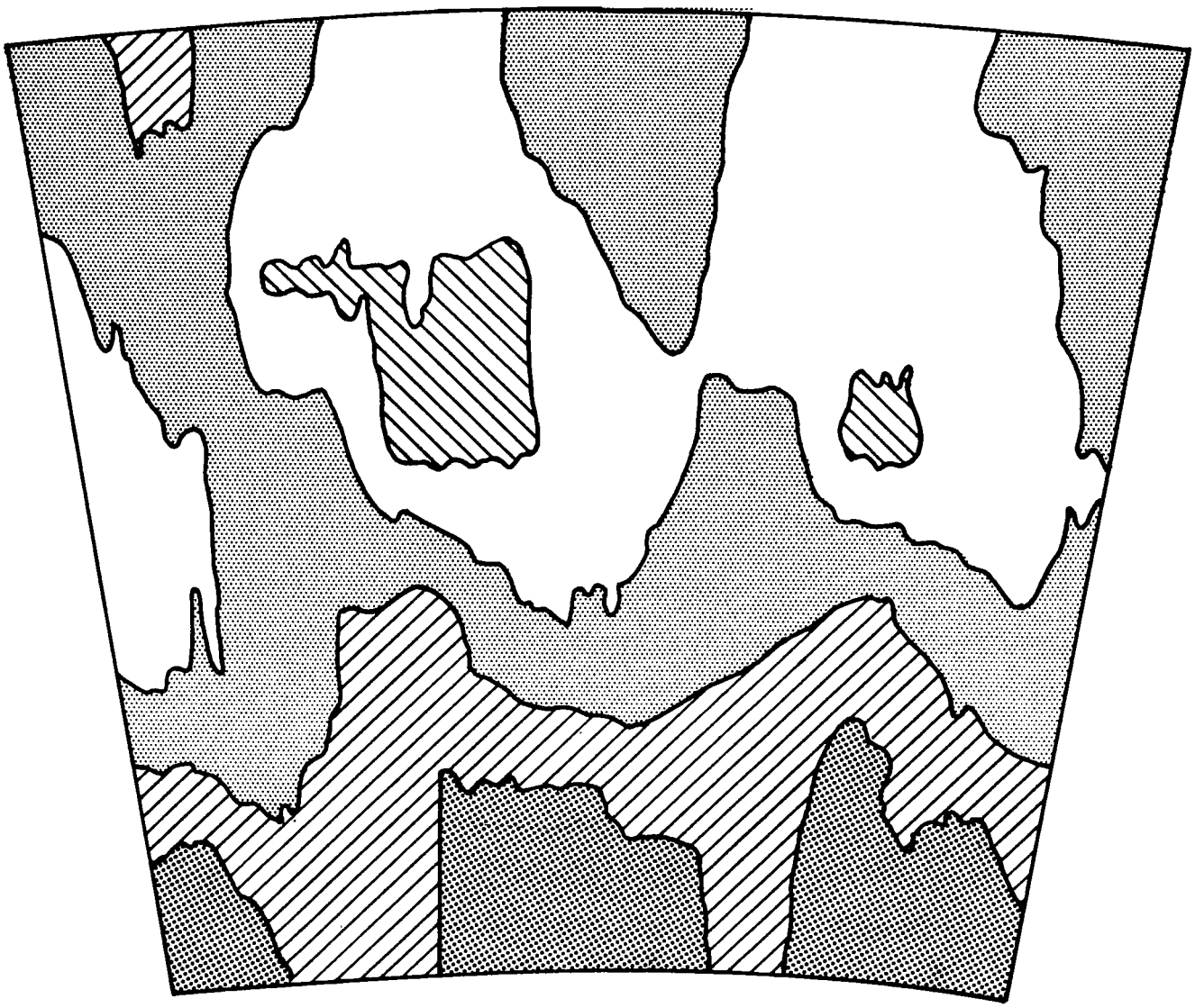

4909 III-19

Figure 19. Turbine stage total efficiency contours for plain rotor blade.

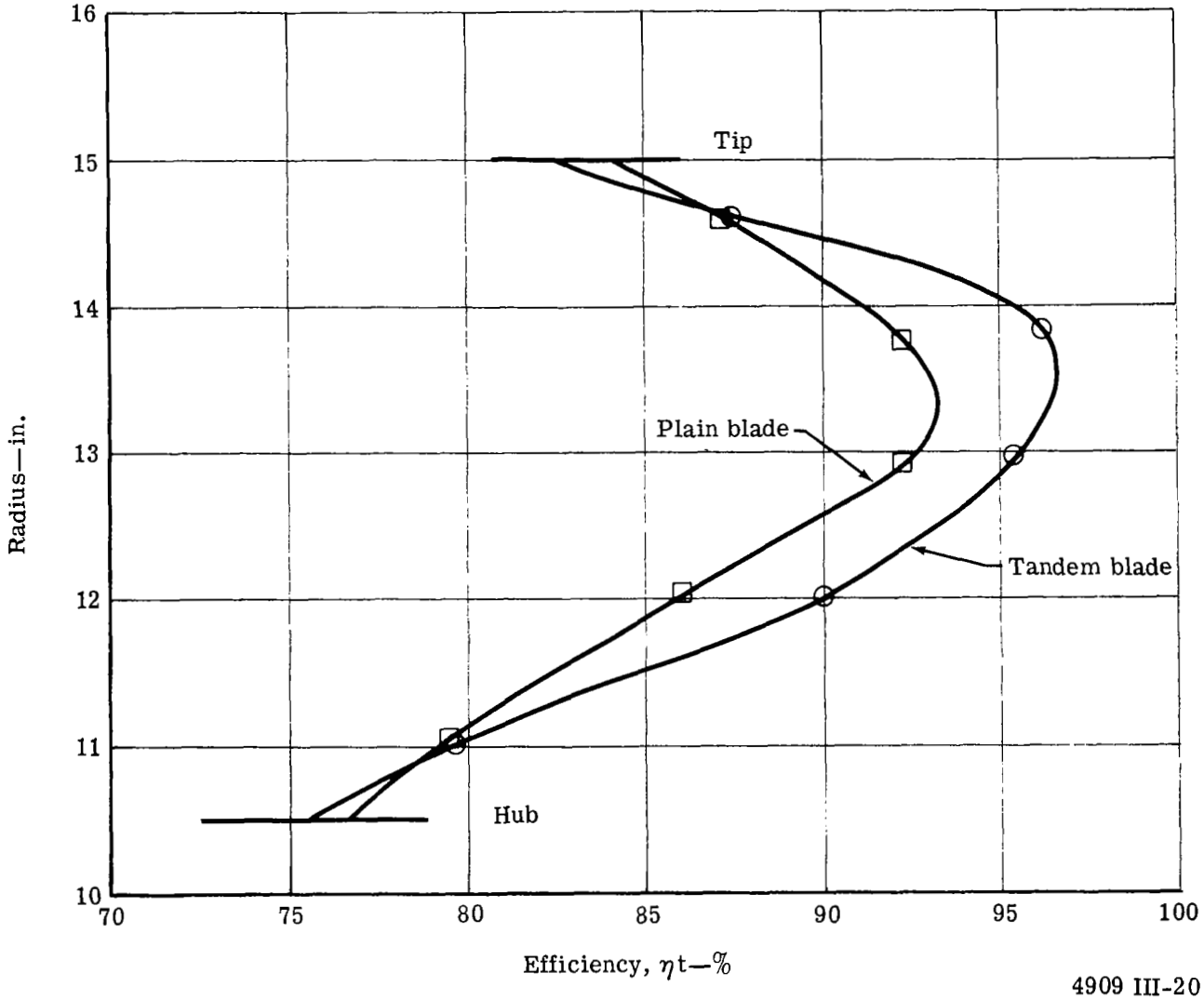

Figure 20. Comparison of radial distribution of efficiency of station 5 for plain blade and tandem blade turbines.